

Competition of ferromagnetism and superconductivity in  $\text{Sc}_3\text{InB}$ 

B. Wiendlocha, J. Tobola, and S. Kaprzyk

Faculty of Physics and Applied Computer Science,  
AGH University of Science and Technology, al. Mickiewicza 30, 30-059 Krakow, Poland

D. Fruchart

Laboratoire de Cristallographie, CNRS, BP 166, 38042 Grenoble Cedex 9, France

J. Marcus

Laboratoire d'Etude des Propriétés Electroniques des Solides,  
CNRS, BP 166, 38042 Grenoble Cedex 9, France

We present results of electronic structure calculations for intermetallic perovskite  $\text{Sc}_3\text{InB}$  with Full Potential KKR-LDA method.  $\text{Sc}_3\text{InB}$  is very promising candidate for a new superconductor (related to  $8\text{ K MgNi}_3$ ) and can be regarded as a boron-inserted cubic  $\text{Sc}_3\text{In}$ , which is a high pressure allotropic form of the hexagonal weak ferromagnet  $\text{Sc}_3\text{In}$ . We predict that cubic  $\text{Sc}_3\text{In}$  can be also magnetic, whereas  $\text{Sc}_3\text{InB}$  having large DOS in the vicinity of  $E_F$  exhibits non-magnetic ground state. Estimation of the electron-phonon coupling for  $\text{Sc}_3\text{InB}$  gives  $\lambda \approx 1$ . Furthermore, the effect of vacancy in  $\text{Sc}_3\text{InB}_{1-x}$  and antisite disorder in  $\text{Sc}_3(\text{In-B})$  on critical parameters is also discussed in view of KKR-CPA method. All theoretical results support possibility of the superconductivity onset in  $\text{Sc}_3\text{InB}$ . Preliminary experimental measurements established the transition temperature close to 4.5 K, with a very abrupt change in susceptibility and a correlated drop of the resistivity when cooling down.

PACS numbers: 74.10.+v, 74.25.Jb, 74.25.Kc, 74.62.Dh, 74.70.Ad, 75.50.Ce

## I. INTRODUCTION

Recent discovery of superconductivity in the intermetallic perovskite  $\text{MgNi}_3$  [1] with  $T_c \approx 8\text{ K}$  was a great surprise due to large Ni contents and this compound was rather expected to be near ferromagnetic critical point [2]. It was established that electron-phonon mechanism is responsible for superconductivity in this material, but few details are still not clear. NMR  $T_1$  relaxation time experiments [3] or specific heat measurements [4] have resulted in typical behaviors, supporting s-wave type pairing with electron-phonon coupling constant  $\lambda \approx 0.8$ . Conversely, rather unconventional behaviors have been observed in other experiments (e.g. increase of critical temperature with pressure [5] or unusual low temperature behavior of London penetration depth  $\lambda_L(T)$  [6]), which can be partly connected with spin fluctuations likely appearing due to vicinity of ferromagnetism. Moreover, complex dynamical properties of this superconductor, as e.g. soft mode behaviors and instability of Ni vibrations [7], [8], make its theoretical analysis quite cumbersome.

In this paper we report on predictions of superconductivity in related  $\text{Sc}_3\text{InB}$  compound, which also seems to be close to magnetism limit due to weak ferromagnetic properties of  $\text{Sc}_3\text{In}$ . It was already revealed that  $\text{Sc}_3\text{InB}$

crystallizes in a perovskite structure (space group  $\text{Pm-}3m$ ,  $\text{CaTiO}_3$  type) with lattice constant  $a = 4.56\text{ \AA}$  [10]. However, the same number of valence electrons of boron and indium elements may give rise to lattice instabilities and In/B antisite defects are plausible.

## II. THEORETICAL STUDY

Electronic structure calculations were performed by Full Potential KKR method [11], [12] within the LDA framework employing von Barth-Hedin formula for the exchange-correlation potential. Figure 1 presents electron density of states (DOS) in  $\text{Sc}_3\text{InB}$  compound. The Fermi level ( $E_F$ ) is located on the decreasing slope of large DOS peak with the  $n(E_F)$  value being as large as  $\approx 90$  states/Ry. The main contributions can be attributed to Sc (d-states) and In (p-states) (see Tab. I). Noteworthy, appearance of a large DOS peak close to  $E_F$ , coming essentially from transition metal Ni d-states, was also characteristic of electronic structure of  $\text{MgNi}_3$  (Mg contribution was negligible) [2], [9]. The  $\text{Sc}_3\text{InB}$  case is not similar, since In plays more active role in formation of electronic states near  $E_F$  due to one electron more on p-shell.

a. Predictions of superconductivity in  $\text{Sc}_3\text{InB}$  The electron-phonon coupling strength was estimated by calculating McMillan-Hopfield parameters [13] from Gaspari-Gyor'y formulas [14] [16] within Rigid Muffin-Tin Approximation (RM TA). The electron-phonon coupling constant was then calculated from relation:  $\lambda = \sum_i \frac{m_i}{M_i} \frac{\hbar^2}{2} \frac{1}{\omega_i}$ , where  $i$  corresponds to atoms in the

email: bartekw@fatcat.ftjagh.edu.pl;

This work was presented at the European Conference Physics of Magnetism '05, 24-27.06.2005, Poznan, Poland.

TABLE I: Properties of  $\text{Sc}_3\text{InB}$ .  $n(E_F)$  is given in  $\text{Ry}^{-1}/\text{atom}$ ,  $n_s(E_F)$  in  $\text{mRy}/a_B^2/\text{atom}$ ,  $\Delta$  in  $\text{meV}$ ,  $Mh_i^2$  in  $\text{mRy}/a_B^2$ .

Atom	$n(E_F)$	$n_s(E_F)$	$n_p(E_F)$	$n_d(E_F)$	$n_f(E_F)$	$sp$	$pd$	$df$	$P$	$h!^2i$	$M h!^2i$	
Sc	20.26	0.06	2.34	16.98	0.88	18.6	0.0	4.7	13.3	18.5	75.7	0.74
In	18.28	0.04	16.72	1.16	0.32	1.5	0.0	1.5	0.0	18.5	193.4	0.01
B	6.72	0.02	5.92	0.42	0.36	34.3	0.0	34.3	0.0	58.3	180.9	0.19

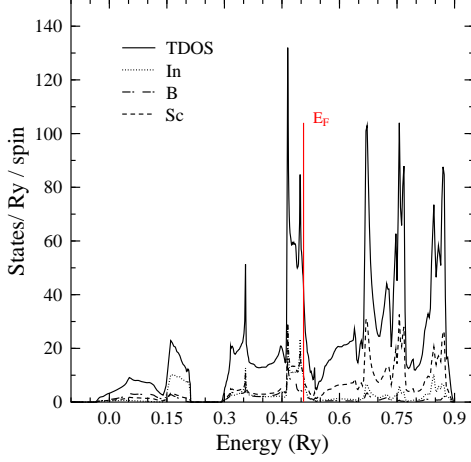


FIG. 1: Total electron DOS in  $\text{Sc}_3\text{InB}$ .

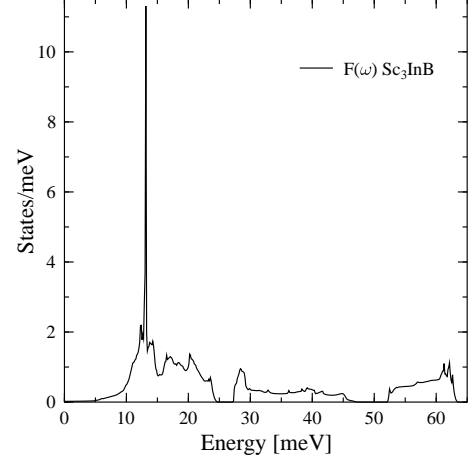


FIG. 2: Phonon DOS in  $\text{Sc}_3\text{InB}$ .

unit cell. The  $h_i^2$  parameter was derived from phonon DOS  $F(\omega)$  [22], computed for minimum energy lattice constant  $a_0 = 8.610 a_B$  ( $1 a_B = 0.529 \text{ \AA}$ ) within Density Functional Perturbation Theory, using the PW scf package [17].

In order to take into account the markedly different masses of Sc, In and B atoms, phonon spectrum was analyzed while focusing on two parts: low frequency region with predominantly In and Sc modes (peak at 13 meV comes from acoustic In modes) and high frequency region with B vibrations (above 50 meV). Noteworthy, similar separation of phonon DOS was earlier observed experimentally in  $\text{MgCNi}_3$  [8]. Values of  $h_i^2$  used next to estimate  $\Delta$ , were calculated separately for both regions (with cut line at 50 meV):  $h_i^2$  for Sc and In are taken to be equal, and represent the low frequency part, while  $h_B^2$  was taken from high frequency part of the spectrum. Results and estimation of  $\Delta$  are presented in Table I, total electron-phonon coupling constant is  $\lambda = 0.94$ .

Using McMillan formula [13] for critical temperature and applying typical value of Coulomb pseudopotential  $\mu^* = 0.13$ , we got  $T_c = 12 \text{ K}$  (we used  $h_i^2 = 1.2$  with  $h_B^2 = 19.5 \text{ meV}$  instead of  $h_B^2 = 1.45$  in McMillan formula in practical computations). Both  $\lambda$  and  $T_c$  values belong to moderate regime of superconducting parameters within the BCS model, and are higher than in  $\text{MgCNi}_3$ .

We can also notice advantageous trend of electron-phonon coupling in  $\text{Sc}_3\text{InB}$  if comparing with  $\text{MgCNi}_3$  superconductor. Our KKR calculations for  $\text{MgCNi}_3$  showed that Ni has the largest McMillan Hopfield pa-

rameter:  $Ni = 20 \text{ mRy}/a_B^2$  with respect to other atoms ( $C = 9 \text{ mRy}/a_B^2$ ,  $Mg$  - negligible). The value of  $Sc$  in  $\text{Sc}_3\text{InB}$  is similar to  $Ni$  in  $\text{MgCNi}_3$  but  $B$  is over three times larger than  $C$  (both In and Mg contributions are much smaller). In view of recent  $C$  isotope effect measurements [18] (very large  $\alpha = 0.54$  coefficient) and bearing in mind a particular sensitivity of  $T_c$  on the carbon concentration, one can conclude that both C and Ni sublattices are important in superconductivity of  $\text{MgCNi}_3$ . In view of these criterion  $T_c$  in  $\text{Sc}_3\text{InB}$  can be expected higher than in  $\text{MgCNi}_3$ .

b. Magnetic properties of  $\text{Sc}_3\text{In}$ . It seems that instability towards magnetism may also be present in  $\text{Sc}_3\text{InB}_{1-x}$  compound. First, we have studied electronic structure of both allotropic phases of  $\text{Sc}_3\text{In}$ . The hexagonal compound ( $\text{Ni}_3\text{Sn}$ -type,  $a = 6.42 \text{ \AA}$ ,  $c = 5.18 \text{ \AA}$  [10]) is well known weak itinerant ferromagnet, while the cubic compound ( $\text{Cu}_3\text{Au}$ -type,  $a = 4.46 \text{ \AA}$ , synthesized under high pressure [10]) has not been yet investigated to our knowledge. Present KKR calculations showed that both allotropic forms of  $\text{Sc}_3\text{In}$  should exhibit magnetic ground state supported by magnetic moment on Sc atoms, i.e.  $0.26 \mu_B$  (hexagonal phase) and  $0.27 \mu_B$  (cubic phase). We should remind that experimentally observed magnetic moment is much weaker ( $0.05 \mu_B/\text{Sc}$  in hexagonal phase), as already underlined in the previous LAPW calculations [19]. Besides, the superconductor-to-ferromagnet transition can appear in  $\text{Sc}_3\text{InB}_{1-x}$  if varying B content (KKR-CPA computations are in progress). Thus, as already suggested in

MgCNi<sub>3</sub> [2], [7] one can expect that the proximity of ferromagnetic quantum critical point (resulting in enhanced spin fluctuations) may probably compete with superconductivity.

### III. EXPERIMENTAL ANALYSES

A 1.5 g sample was first prepared by arc melting under high purity argon atmosphere (99.9995) starting from the appropriate proportions of the elements (purity > 99.95) to obtain the Sc<sub>3</sub>InB formula. The resulting small ingot was melted several times in order to insure homogeneity. Pieces of the ingots were made by using a metal mortar, and inspection by using an optical microscope reveals the bright and homogeneous aspect of the fractured surfaces. Then, XRD patterns were recorded at room temperature (Cu) using a Bragg-Brentano diffractometer equipped with a backscattering pyrolytic graphite monochromator. The diffraction pattern reveals the presence of a dominant amount of cubic phase with the addition of a minor impurity. Probably because no annealing procedure was applied, the crystallized state of the sample was not of the best and no effective crystal structure refinement was applied. However using the PowderCell code [20], the two main phases were clearly identified and a rough determination of the cell parameters was made possible. The main phase (70 % vol.) is simple cubic of perovskite type of structure and the second one (30 % vol.) is hexagonal of Ni<sub>2</sub>In type of structure (space group P6<sub>3</sub>/mmc). Accounting for the large difference in between the scattering lengths of the p-elements B and In, an estimate of the composition of the main phase was made. All the results are displayed on Table II.

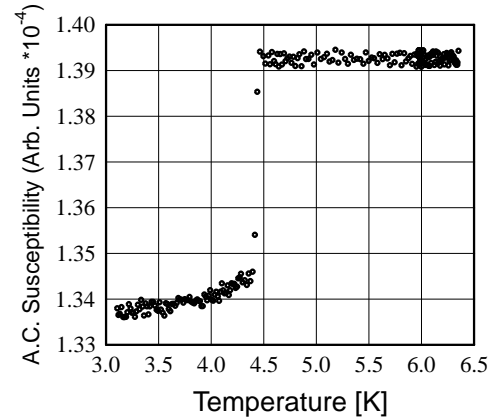
TABLE II: Structure analysis of the material synthesized with the nominal composition Sc<sub>3</sub>InB.

Compound	Type	Cell parameters [Å]			Composition
Sc <sub>3</sub> InB					
(70 % vol.)	CaTiO <sub>3</sub>	4.66	4.66	4.66	Sc <sub>3</sub> In <sub>1.3</sub> B <sub>0.7</sub>
Sc <sub>2</sub> In					
(30 % vol.)	Ni <sub>2</sub> In	5.05	5.05	6.30	Sc <sub>2</sub> In

The best agreement for the main phase composition leads to consider that the p-elements B and In are neither fully ordered nor randomly distributed, with about 0.70 In and 0.30 B atom on the 1a site, then 0.65 In and 0.35 B atom on the 1b site of the space group Pm-3m. Consideration for such a type of atomic disordering was already reported in literature [21]. Both the compositions of the two compounds (3-1-1 and 2-1) confirm that boron is a difficult element to combine, thus the remaining boron should be detected in the XRD pattern, unless it is difficult to evidence effectively as a very light and often poorly crystallized element.

Susceptibility and resistivity measurements were made using a a.c. susceptometer in temperature ranging from 50 to 2 K. Millimeter sized pieces of the ingot were measured successively and lead to the same results. A typical record is shown on Figure 3, thus revealing the onset of a superconducting state down to 4.4 K, the transition being very sharp with no detectable hysteresis loop. A change in the resistivity trace was also observed simultaneously.

FIG. 3: A.c. susceptibility trace revealing the transition to superconducting state.



Unexpectedly, the rest of the ingot and the small pieces rapidly change their brittle and bright aspects after several hours left in ambient atmosphere. Besides, a tentative to melt twice the main parts of the initial ingot was made, but at this time no evidence for any superconducting transition was found. Then, several new syntheses were undertaken, thus operating as possible similarly as for the first one procedure. Again, the new ingots we obtained do not display any transition down to 2 K. As revealed by the theoretical derivations (see below), the superconducting state and the related transition look fairly dependant on the p-element ordering and the stoichiometry in the 1a and 1b sites. So, we anticipate that during and after the different melts, the new samples do not exhibit the same atom ordering as it was resulting from the first attempt. New syntheses are now scheduled to be undertaken using different methods and techniques in order to achieve optimized compounds.

Because of experimental problems with synthesis, effect of boron site vacancy on electronic structure near  $E_F$  and superconducting properties was simulated using KKR method with coherent potential approximation (CPA). We have found significant change in  $\chi$  values not only for B, but also for Sc, i.e. for 7% boron deficiency (Sc<sub>3</sub>InB<sub>0.93</sub>), employing the same values of  $\hbar^2 \chi_i$ , total decreased over 30% to 0.62, which resulted in  $T_c \approx 4$  K. In Sc<sub>3</sub>InB<sub>0.85</sub> coupling constant is so small ( $\approx 0.4$ ),  $T_c < 0.5$  K seems to be below the standard low temperature measurements. Similar decrease (but less rapid than in the case of B vacancy) of critical parameters was detected from KKR-CPA analysis when antisite In/B disorder increased.

- 
- [1] T. He et al., *Nature*, 411, 54 (2001).
- [2] H. Rosner, R. W. Hecht, M. D. Johannes, W. E. Pickett, E. Tosatti, *Phys. Rev. Lett.* 88, 027001 (2002).
- [3] P. M. Singer, T. Imai, T. He, M. A. Hayward, R. J. Cava, *Phys. Rev. Lett.* 87, 257601 (2001).
- [4] J. Y. Lin et al., *Phys. Rev. B*, 67, 52501 (2003).
- [5] T. G. Kumary et al., *Phys. Rev. B*, 66, 064510 (2002).
- [6] R. Prozorov, A. Snezhko, T. He, R. J. Cava, *Phys. Rev. B*, 68, 180502 (2003).
- [7] A. Yu. Ignatov, S. Y. Savrasov, T. A. Tyson, *Phys. Rev. B*, 68, 220504 (2003).
- [8] R. Heid, B. Renker, H. Schober, P. Adelmann, D. Ernst, K. P. Bohnen, *Phys. Rev. B* 69, 092511 (2004).
- [9] A. Szajek, *J. Phys.: Condens. Matter* 13, 595 (2001).
- [10] P. Villars, L. Calvert, *Pearson's Handbook on Intermetallic Phases* (ASM International, Metals Park, Ohio, 1991).
- [11] A. Bansil, S. K. Przyby, P. E. M. Ijzereids, and J. Tobola, *Phys. Rev. B* 60, 13396 (1999).
- [12] T. Stopa, S. K. Przyby, and J. Tobola, *J. Phys.: Cond. Matter* 16, 4921 (2004).
- [13] W. L. McMillan, *Phys. Rev.* 167, 331 (1968).
- [14] G. Gaspari and B. Gyorffy, *Phys. Rev. Lett.* 28, 801 (1972).
- [15] B. M. Klein and D. A. Papaconstantopoulos, *Phys. Rev. Lett.* 32, 1193 (1974).
- [16] W. E. Pickett, *Phys. Rev. B* 25, 745 (1982).
- [17] S. Baroni, A. Dal Corso, S. de Gironcoli and P. Gian-nozzi, [www.pwscf.org](http://www.pwscf.org).
- [18] T. Klimczuk and R. J. Cava, *Phys. Rev. B* 70, 212514 (2004).
- [19] A. Aguayo and D. J. Singh, *Phys. Rev. B* 66, 20401 (2002).
- [20] W. Kraus and G. Nolze, *PowderCell*, Fed. Inst. for Mat. Res. and Testing, Berlin, Germany 112 (1999).
- [21] H. Holleck, *J. Less Common Met.* 52, 167 (1977).
- [22] Definition:  $\hbar^n i \bar{R}^{n-1} F^{(n-1)}(\omega) d\omega = \hbar^{n-1} F^{(n-1)}(\omega) d\omega$ , if  $F^{(n-1)}(\omega)$  is the electron-phonon interaction coefficient.